Theory of the Raman spectra of the Shastry-Sutherland antiferromagnet $SrCu_2(BO_3)_2$ doped with nonmagnetic impurities

S. Capponi* and D. Poilblanc
Université de Toulouse; UPS; Laboratoire de Physique Théorique (IRSAMC); F-31062 Toulouse, France and CNRS; LPT (IRSAMC); F-31062 Toulouse, France

F. Mila
Institute of Theoretical Physics, Ecole Polytechnique Fédérale de Lausanne, 1015 Lausanne, Switzerland
(Received 13 February 2009; revised manuscript received 11 August 2009; published 15 September 2009)

Controlled doping of $SrCu_2(BO_3)_2$, a faithful realization of the Heisenberg spin-1/2 antiferromagnet on the Shastry-Sutherland lattice, with nonmagnetic impurities generates bound states below the spin gap. These bound states and their symmetry properties are investigated by exact diagonalization of small clusters and within a simple effective model describing a spinon submitted to an attractive extended potential. It is shown that Raman spectroscopy is a unique technique to probe these bound states. Quantitative theoretical Raman spectra are numerically obtained.

DOI: 10.1103/PhysRevB.80.094407 PACS number(s): 75.10.Jm, 75.40.Gb

I. INTRODUCTION AND MOTIVATIONS

$SrCu_2(BO_3)_2$ is an experimental realization of a spin-1/2 antiferromagnet living on the two-dimensional (2D) Shastry-Sutherland lattice (SSL). Its properties can be well described with the Heisenberg model

$$\mathcal{H} = J\sum_{nn} \mathbf{S}_i \cdot \mathbf{S}_j + J'\sum_{nnn} \mathbf{S}_i \cdot \mathbf{S}_j, \tag{1}$$

where J (respectively, J') is the exchange within (respectively, between) dimers. The experimental compound has a ratio $\alpha = J'/J$ slightly above[1] 0.6. The SSL has been first introduced theoretically as an example of a 2D antiferromagnet whose ground state (GS) for small enough α is exactly known:[2] it is simply the product of singlets on each dimer up to[1] $\alpha \simeq 0.7$. Indeed, experiments on $SrCu_2(BO_3)_2$ indicate a finite spin gap. For larger α, a more usual 2D Néel-ordered phase is stabilized, possibly with an intermediate plaquette phase. Previous Raman experiments on this compound[3] indicate that some structure in the spectrum can only be explained by taking into account a realistic model, including for instance Dzyaloshinski-Moriya (DM) interactions.[4] However, these DM terms are too small to have any sizeable effects on the low-energy Raman spectra[5] discussed here and thus will be neglected hereafter. Our goal will be to show that, within a simple Heisenberg model, doping nonmagnetic impurities generates new spectroscopic signatures below the two-magnon continuum whose features should persist in a more realistic model.[5]

$SrCu_2(BO_3)_2$ is a Mott insulator and its doping with mobile carriers is predicted to lead to superconductivity.[6] In this paper, we shall rather consider the controlled doping of $SrCu_2(BO_3)_2$ with nonmagnetic *static* impurities such as zinc or magnesium atoms substituted for copper atoms on a very small fraction of the N lattice sites. Such atoms acting as vacant sites provide accurate local real-space probes (which can be considered as independent for low enough impurity concentration). As known in strongly correlated systems, a small doping of the parent compound can bring crucial informations about its intrinsic properties.[7] Substituting Cu with nonmagnetic Mg impurities has been recently performed.[8,9] Neutron-scattering experiments[8] have then shown the appearance of new magnetic excitations into the singlet-triplet gap. Here, we shall focus on Raman-spectroscopic techniques which, by probing $\Delta S = 0$ excitations using light scattering, offer a unique way to identify the local response to a doped impurity. In particular, we will show that transitions between different $S = 1/2$ bound states can be identified in the Raman spectra. Such features can be interpreted within a simple phenomenological model describing the attractive potential between a liberated spinon and the impurity (vacant site).

II. THEORETICAL FRAMEWORK

A. Raman scattering

The theory of Raman light scattering is most simple when the photon energy is much smaller than the Mott gap. In such a case, it is legitimate to use the Loudon-Fleury approximation and the Raman operator reads

$$\mathcal{R} = \sum_{nn} \gamma(\mathbf{e}_{in} \cdot \mathbf{d}_{ij})(\mathbf{e}_{out} \cdot \mathbf{d}_{ij})\mathbf{S}_i \cdot \mathbf{S}_j + \sum_{nnn} \gamma'(\mathbf{e}_{in} \cdot \mathbf{d}_{ij})(\mathbf{e}_{out} \cdot \mathbf{d}_{ij})\mathbf{S}_i \cdot \mathbf{S}_j, \tag{2}$$

where $\mathbf{e}_{in}$ and $\mathbf{e}_{out}$ are the polarization vectors of the incoming and scattered light, and $\mathbf{d}_{ij}$ is the unit vector connecting two sites i and j. This operator only couples to zero-momentum singlet excitations. In principle, the coupling constants γ and γ' could depend on the exchange values,[10] although such a dependence is neglected in most studies. However, some simplifications occur for an $(a'b')$ polarization (see Fig. 1): indeed, in this case, the geometry of the compound implies that only the J' bonds contribute to the Raman operator. Moreover, the dominant intensity occurs when triplets can be created on dimer bonds which, in contrast, is not allowed in (ab) polarization.[11,12] In the follow-

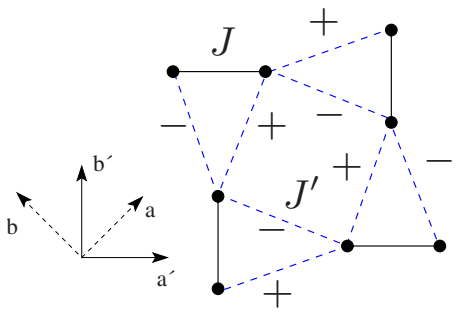

FIG. 1. (Color online) Shastry-Sutherland lattice. ± signs correspond to Raman coupling in the $(a'b')$ polarization case.

ing, we will restrict to this polarization where all Raman coupling constants are equal up to a sign (given in Fig. 1).

At zero temperature, the Raman intensity is given by the dynamical correlations of the Raman operator

$$\mathcal{I}_R(\omega) = -\frac{1}{\pi}\mathrm{Im}\langle\Psi_0|\mathcal{R}\frac{1}{\omega - \mathcal{H} + i\varepsilon}\mathcal{R}|\Psi_0\rangle$$
$$= \sum_n |\langle n|\mathcal{R}|\Psi_0\rangle|^2\ \delta[\omega - (E_n - E_0)], \qquad (3)$$

where $|\Psi_0\rangle$ is the GS of the system and the sum runs over the excited states $|n\rangle$ with energy E_n. Note that because of the symmetry of the Raman operator, only singlet states with zero momentum contribute. Moreover, in the chosen polarization, only states which are odd with respect to reflections along a' or b' axis give a signal.

B. Results for the pure compound

As studied in Ref. 11, the Raman spectrum of the undoped material shows four sharp peaks at 1.25, 1.9, 2.3, and 2.9 times the spin gap Δ_{01}. Naively, one would expect the Raman spectrum to start at the two-magnon continuum (i.e., twice the spin gap) since it is a singlet operator. In fact, a singlet bound state made of two triplets does exist on this lattice[12] and was identified as the low-energy state.[11] The first two peaks are attributed to two-triplet bound states, while the two others are interpreted in terms of three-particle excitations. Although the high-intensity peaks are above the two-magnon continuum (starting at $2\Delta_{01}$), the very small magnon dispersion leads to a very narrow continuum so that the two higher-energy peaks are observable.

In Fig. 2, we present our exact-diagonalization (ED) spectra for various α. As expected, for small α, the finite-size effects are rather weak due to the large energy scales (i.e., short correlation lengths), so that results are almost identical on $N=16$ and $N=32$ clusters. Clearly, spectral weight is present below the two-magnon threshold. On the other hand, for larger α, finite-size effects become sizeable so that a direct comparison with experimental values is difficult. However, one can still notice spectral weight well below the two-magnon continuum, corresponding to the above mentioned singlet bound states. Note also that, for $N=32$, the first peak is located at an energy $1.2\Delta_{01}$ as seen in experiments.

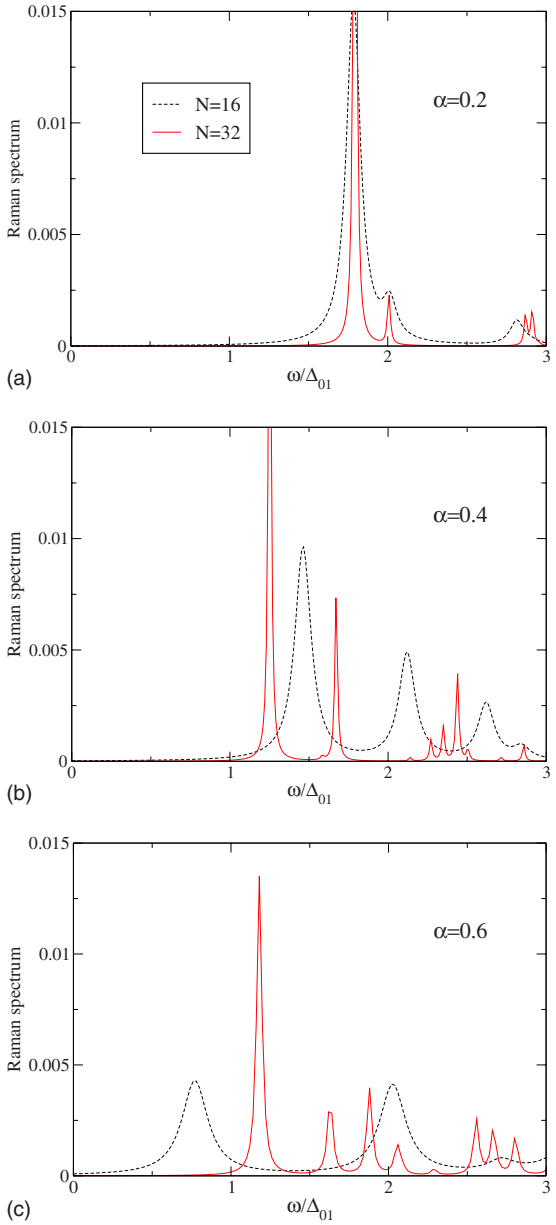

FIG. 2. (Color online) Raman spectra for pure SSL for various α on $N=16$ and 32 clusters. The spin gap Δ_{01} [$\sim$0.95, 0.80, 0.50 J in (a), (b), and (c), respectively] is used as a unit of frequency. An artificial width $\varepsilon=0.01$ has been given to the delta peaks.

C. Results for the doped case

We now turn to the doped case for which additional low-energy states appear. We shall assume a small enough impurity concentration so that a single impurity description becomes legitimate. Using a variational approach, El Shawish and Bonča[13] have proposed anisotropic spin-polaronic states with a finite spatial extension around the impurity. Adding a single impurity (i.e., creating a vacant site by removing a spin) indeed generates a polarization 1/2 that will distribute around the impurity. On Fig. 3, we show the GS magnetization pattern computed exactly on a $N=32$ cluster with one impurity. The local polarization oscillates from one site to the other similar to the Friedel oscillations reported around a

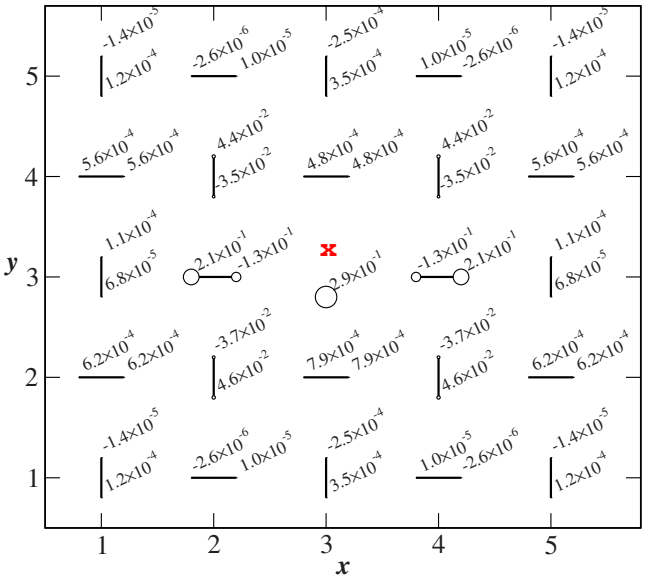

FIG. 3. (Color online) Magnetization pattern around the impurity (marked as x) on $N=32$ SSL for $\alpha=0.6$ ($S_z^{tot}=1/2$). Periodic boundary conditions are used. Since the reflection around the b' axis is still a good symmetry, we observe identical values on both sides.

localized triplet in the 1/8 plateau.[14] Note however that each strong dimer has a global positive polarization. Our results are in good agreement[15] with the GS variational estimate of Ref. 13. These authors have also found low-energy states appearing below the undoped spin gap. Since these states are well localized, we expect that finite-size calculations can provide accurate results for these excitations as well. In particular, we expect a much better accuracy than in the pure case.

The existence of several $S_z=1/2$ low-energy states has led to various experimental signatures: by flipping spins, they can be observed in neutron experiment[8] (which is sensitive to $\Delta S=1$ transitions); moreover, since these states can be connected by $\Delta S=0$ transitions, they are also expected to be Raman active, which is the main purpose of our study. Figure 4 shows the Raman spectra obtained by exact diagonalizations on $N=16$ and 32 clusters with one impurity for various α. The spectra are plotted as a function of ω/Δ_{01}, where the spin gap of the pure sample Δ_{01} is very close to the spin gap $\Delta_{\frac{1}{2}\frac{3}{2}}$ in the doped cluster (both computed on the largest cluster). In the small α regime, all energy scales are well separated and finite-size effects are negligible so that one can understand all features. For the pure system, as discussed above, there is a bound state below $2\Delta_{01}$ and then another peak at $2\Delta_{01}$ corresponding to a singlet excitation made of two distant triplets. Since the triplets have a small dispersion, there is no continuum above. In the presence of a single impurity, these features still represent much of the spectral weight but, in addition, new peaks appear below the spin gap. Namely, one can make a singlet excitation by creating a triplet in the bulk while flipping the polarization cloud (so that the number of such peaks scales as the number of dimers $N_d=\frac{N}{2}-1$). Moreover, there is a possibility to form a bound states of these two excitations, which can even lower the

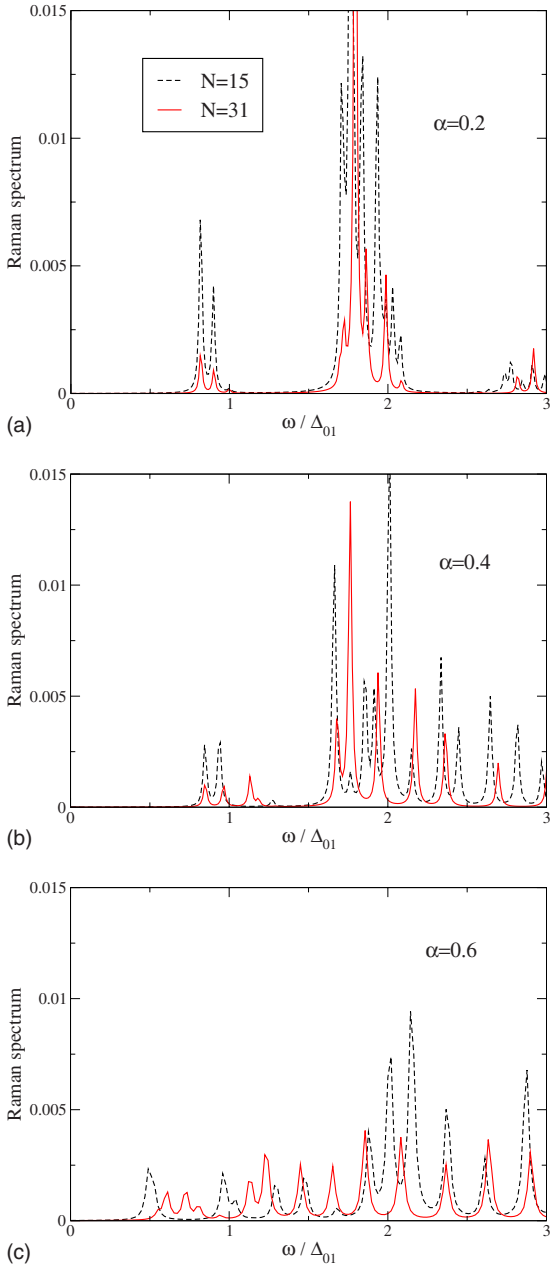

FIG. 4. (Color online) Raman spectra for SSL doped with a single nonmagnetic impurity for various α on $N=16$ and 32 clusters. The spin gap Δ_{01} [~ 0.95, 0.80, 0.50 J in (a), (b), and (c), respectively] is used as a unit of frequency. An artificial width $\varepsilon=0.01$ has been given to the delta peaks.

energy below the spin gap (see Fig. 4), as found numerically. Another feature of this additional spectral weight is that it scales with the concentration of impurity, i.e., is reduced by ~ 2 when doubling the system size.

In order to be more quantitative, we compare these bound-state energies with the variational results of Ref. 13 for $\alpha=0.62$ where the two lowest $S=1/2$ states have excitation energies 0.238 and 0.264 J, while the undoped spin gap is 0.450 J. In our exact calculations on $N=32$ cluster for the same α, we find that the three lowest excitations have a total spin 1/2 and are located at 0.217, 0.245, and 0.268 J, while the spin gap is 0.479 J in good agreement with these varia-

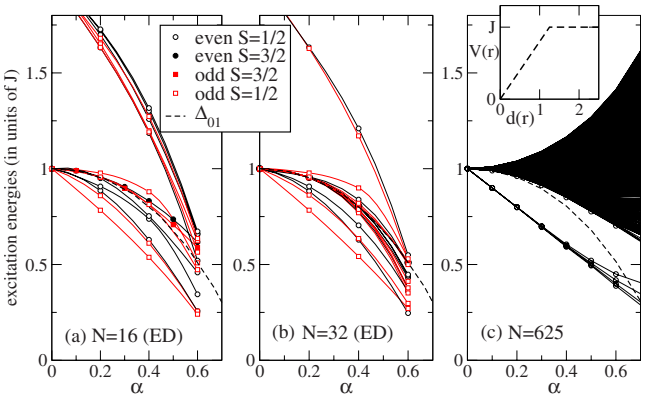

FIG. 5. (Color online) Low-energy $S=1/2$ excitations vs α. The dashed line indicates the perturbative estimation of the spin gap (see text). [(a)–(b)] Microscopic model on $N=16$ and 32 SSL. The states are classified according to their reflection symmetry. The two lowest $S=3/2$ states also shown give the onset of the continuum. (c) Effective model (see inset for a schematic plot of the effective potential) on a $N=625$ square lattice of dimers for which finite-size effects are not visible.

tional results, except that we have an additional low-energy state. Concerning their Raman signatures, one has to discuss their symmetry properties: in the presence of a single impurity, the translation symmetry is lost and only one reflection along dimers (i.e., along a' or b') remain. Since the Raman operator is odd with respect to this reflection, a simple inspection at the odd/even character of these excited states allow to determine if they are/are not Raman active. In Figs. 5(a) and 5(b), we have indicated all even and odd $S_{tot}=1/2$ states below the first $S_{tot}=3/2$ state on $N=16$ and 32 clusters. A careful comparison with the Raman spectra does confirm that only states with $S_{tot}=1/2$ and which are odd w.r.t. reflection give Raman peaks at low energy.

III. EFFECTIVE MODEL FOR THE BOUND STATES

Interestingly, a phenomenological description of these bound states can be given similarly to the case of doped quasi-one-dimensional $CuGeO_3$.[16,17] For $J'=0$, a free $S=1/2$ (spinon) is located next to the vacant site, on the broken dimer bond. Switching on J' allows this spinon to delocalize with a hopping term of order $(J')^2/4J$. However, each time the spinon hops one dimer away from the impurity, a strong bond is broken resulting in an additional "string" energy cost $\sim(J-J')$. Therefore, the physics is similar to a particle in a linear potential and bound states can occur. Of course, when the string energy exceeds the spin gap, the whole picture breaks down and the spinon can "escape" in a flat potential by the spontaneous creation of a spinon-antispinon pair out of the vacuum. We have considered this effective quantum-mechanical model on an effective square lattice for one particle allowed to hop with amplitude $\alpha^2/4$ on its neighboring sites (except between the impurity dimer and the neighboring dimer facing the vacant site) and with a potential energy equals to $V(r)=J\min[(1-\alpha)d(r),1]$, where d is the Manhattan distance from the impurity dimer. This one-particle problem can be easily solved on large clusters and its spectrum is presented on Fig. 5(c). For vanishing J', the low-energy $S=1/2$ spectrum is extensively degenerate: the $N_d=\frac{N}{2}-1$ triplets of excitation energy J located on the remaining bonds can be combined with the impurity spin in total $S=1/2$ states (degenerate with their $S=3/2$ counterparts not described by the model). The next set of states which appears at energy $2J$ (corresponding to two isolated triplets) and above are also not described by the effective model. Switching on J' lifts the degeneracy of the first group of N_d $S=1/2$ states resulting in a rich spectrum well described by the effective model for which the $N\to\infty$ limit can be taken. Common features are observed both in the microscopic and the effective models such as (a) bound states due to the short-range stringlike part of the potential and (b) a continuum of $S=1/2$ excitations above the spin gap [given in Figs. 5(a) and 5(b) by the lowest $S=3/2$ state]. In fact, the estimation of the spin gap from high-order perturbation,[18] $\Delta_{01}=J(1-\alpha^2-\frac{1}{2}\alpha^3-\frac{1}{8}\alpha^4)$, agrees very well with the ED value obtained on the largest $N=32$ cluster up to $\alpha=0.6$ and with the effective model up to $\alpha=0.3$. For small α, the number of bound states below the spin gap is four: in the effective language, it corresponds to a spinon delocalized on one of the nearest-neighbor dimers of the impurity dimer. The situation for larger α is less clear as many states go down, possibly with stronger finite-size effects on ED data. Still, our numerical data would be compatible with up to 12 bound states, some of them being very close to the spin gap. However, with our choice of polarizations and due to the selection rule, only odd states are Raman active, which gives two (respectively, six) low-energy states for $\alpha\sim0.2$ (respectively, $\alpha\sim0.6$).

IV. FINITE IMPURITY CONCENTRATION

To finish, we quickly address the case of a finite impurity concentration for which a two-impurity effective interaction starts to operate. Since each impurity will create a spin-1/2 polarization around it, it is natural to expect some ordering, possibly at low temperature. For instance, antiferromagnetic (AF) ordering occurs in doped $CuGeO_3$ (Ref. 19) and has been predicted for CaV_4O_9.[20] One can imagine an effective diluted spin-1/2 model with a very small exchange interaction (typically, the overlap between two polarization clouds is exponentially small when the impurities are quite far) and such a model is expected to order at low temperature.

In order to estimate the effective coupling constant between two impurities at site $\mathbf{r}$ and $\mathbf{r}'$, we start from the formula $J_{\text{eff}}=2[E(\uparrow\uparrow)-E(\uparrow\downarrow)]$. Now, $E(\uparrow\uparrow)=\Sigma_{\langle ij\rangle}J_{ij}\langle\vec{S}_i\cdot\vec{S}_j\rangle$, where the expectation value is calculated in the triplet state with two impurities. Choosing the polarization along z, and in order to get an estimate, we can approximate the expectation value by $\langle S_i^z\rangle\langle S_j^z\rangle$. We further approximate the polarization of a given site as the sum of the polarizations coming from the two impurities, which would be true to first order in perturbation, leading to

$$\langle S_{i,1}^z+S_{i,2}^z\rangle\langle S_{j,1}^z+S_{j,2}^z\rangle = \langle S_{i,1}^z\rangle\langle S_{j,1}^z\rangle+\langle S_{i,2}^z\rangle\langle S_{j,2}^z\rangle+\langle S_{i,1}^z\rangle\langle S_{j,2}^z\rangle+\langle S_{i,2}^z\rangle\langle S_{j,1}^z\rangle, \tag{4}$$

where $\langle S_{i,1}^z\rangle$ ($\langle S_{i,2}^z\rangle$) is the average magnetization created at

site i by a single impurity located at $\mathbf{r}$ ($\mathbf{r}'$). The same approximation for the correlation functions of $E(\uparrow\downarrow)$ leads to the same terms with the same sign for the 1–1 and 2–2 terms, and opposite signs for the 1–2 and 2–1 terms. The 1–1 and 2–2 terms will drop from the difference, leading to the formula

$$J_{\text{eff}}(\mathbf{r},\mathbf{r}') = 2\sum_{\langle ij\rangle} J_{ij}(\langle S^z_{i,1}\rangle\langle S^z_{j,2}\rangle + \langle S^z_{i,2}\rangle\langle S^z_{j,1}\rangle). \quad (5)$$

From the polarization shown in Fig. 3, the resulting effective exchange can be obtained by considering various configurations of two impurities. Our results (data not shown) indicate that, when both impurities are located on vertical dimers, the effective interaction decreases very fast and is mostly AF. Since these bonds belong to the same sublattice, the presence of strong frustration can prevent magnetic ordering. On the contrary, when both impurities are located on different dimer types (one vertical and one horizontal), the effective interaction is mostly ferromagnetic, thus competing with the AF and often resulting in a disordered state. Anyhow, if magnetic order occurs, it would be at a temperature much below the effective energy scale, which is already quite small. This argument can be generalized to an arbitrary distribution of impurities. In conclusion, we predict the absence of magnetic ordering, even for quite large doping and at extremely low temperature, which seems compatible with experiments.[9]

V. CONCLUSION

In summary, doping a Shastry-Sutherland lattice with nonmagnetic impurities leads to novel low-energy states below the spin gap, that could be probed by Raman spectroscopy. We have proposed a simple effective model to understand bound-state formation as binding of a spinon to an impurity site. For a particular polarization of light, some of these bound states are Raman active with sizeable spectral weights: two of these bound states are located well below the continuum (and exist for any J'/J), while up to four more bound states could be observed for realistic parameters. Moreover, since the effective interactions between impurities is frustrated, we expect no magnetic ordering down to extremely low temperature.

ACKNOWLEDGMENTS

We acknowledge B. Gaulin for very useful discussions. We thank CALMIP (Toulouse) and IDRIS (Paris) for allocation of cpu time. This work has been supported by the French Research Agency (ANR), the Swiss National Fund, by MaNEP, and the région Midi-Pyrénées through its *Chaire d'excellence Pierre de Fermat*. F.M. also thanks LPT (Toulouse) for hospitality.

*capponi@irsamc.ups-tlse.fr

[1] S. Miyahara and K. Ueda, J. Phys.: Condens. Matter **15**, R327 (2003), and references therein.
[2] B. S. Shastry and B. Sutherland, Physica B & C **108**, 1069 (1981).
[3] A. Gozar, B. S. Dennis, H. Kageyama, and G. Blumberg, Phys. Rev. B **72**, 064405 (2005).
[4] Y. F. Cheng, O. Cépas, P. W. Leung, and T. Ziman, Phys. Rev. B **75**, 144422 (2007); V. V. Mazurenko, S. L. Skornyakov, V. I. Anisimov, and F. Mila, *ibid.* **78**, 195110 (2008).
[5] In the presence of DM interactions, $S>0$ spin states might become Raman active. However, we are not concerned here with such excitations which (i) lie at higher energies than the energy range considered here and (ii) would only carry a small spectral weight. In addition, (iii) a perturbative DM interaction has an even weaker effect on the Raman-active low-energy singlet-like excitations.
[6] B. Sriram Shastry and B. Kumar, Prog. Theor. Phys. **145**, 1 (2002); J. Liu, N. Trivedi, Y. Lee, B. N. Harmon, and J. Schmalian, Phys. Rev. Lett. **99**, 227003 (2007).
[7] S. Sachdev and M. Vojta, Phys. Rev. B **68**, 064419 (2003).
[8] S. Haravifard, S. R. Dunsiger, S. El Shawish, B. D. Gaulin, H. A. Dabkowska, M. T. F. Telling, T. G. Perring, and J. Bonča, Phys. Rev. Lett. **97**, 247206 (2006).
[9] A. A. Aczel, G. J. MacDougall, J. A. Rodriguez, G. M. Luke, P. L. Russo, A. T. Savici, Y. J. Uemura, H. A. Dabkowska, C. R. Wiebe, J. A. Janik, and H. Kageyama, Phys. Rev. B **76**, 214427 (2007).
[10] P. J. Freitas and R. R. P. Singh, Phys. Rev. B **62**, 14113 (2000).
[11] P. Lemmens, M. Grove, M. Fischer, G. Güntherodt, V. N. Kotov, H. Kageyama, K. Onizuka, and Y. Ueda, Phys. Rev. Lett. **85**, 2605 (2000).
[12] C. Knetter, A. Bühler, E. Müller-Hartmann, and G. S. Uhrig, Phys. Rev. Lett. **85**, 3958 (2000).
[13] S. El Shawish and J. Bonča, Phys. Rev. B **74**, 174420 (2006).
[14] K. Kodama, M. Takigawa, M. Horvatic, C. Berthier, H. Kageyama, Y. Ueda, S. Miyahara, F. Becca, and F. Mila, Science **298**, 395 (2002).
[15] For $\alpha=0.62$, the relative error between ground-state energies with a single impurity obtained with ED on $N=32$ or in the variational approach of Ref. 13 is 1.4%.
[16] G. Els, G. S. Uhrig, P. Lemmens, H. Vonberg, P. H. M. van Loosdrecht, G. Guentherodt, O. Fujita, J. Akimitsu, G. Dhalenne, and A. Revcolevschi, Europhys. Lett. **43**, 463 (1998).
[17] D. Augier, E. Sørensen, J. Riera, and D. Poilblanc, Phys. Rev. B **60**, 1075 (1999).
[18] S. Miyahara and K. Ueda, Phys. Rev. Lett. **82**, 3701 (1999).
[19] J.-P. Renard, K. Le Dang, P. Veillet, G. Dhalenne, A. Revcolevschi, and L.-P. Regnault, Europhys. Lett. **30**, 475 (1995).
[20] S. Wessel, B. Normand, M. Sigrist, and S. Haas, Phys. Rev. Lett. **86**, 1086 (2001).